Effect of Endomyocardial Laser Channels on Regional Innervation Shown with ^{125}I-MIBG and Autoradiography

Lynne L. Johnson, MD[1]; Sukumaran Thambar, MD[1]; Tammy Donahay, BS[1]; Michael Dae, MD[2]; and David O. Williams, MD[1]

[1]Rhode Island Hospital, Brown University, Providence, Rhode Island; and [2]University of California at San Francisco, San Francisco, California

The aim of this study was to map regional innervation against regional flow early after laser channel placement using autoradiography in a porcine model. **Methods:** Four juvenile male swine underwent left ventricular mapping using a catheter-based mapping system and laser treatment with 20–30 channels to the mid and distal anterior wall of the left ventricle. Three days later animals were injected with 37 MBq ^{125}I-metaiodobenzylguanidine (MIBG) followed in 3 h with 1,110 MBq ^{99m}Tc-sestamibi; 1 h later the animals were killed. Hearts were removed, perfusion fixed, and sliced into 1-cm slices. The slices best showing laser holes were selected, and circumferential sections were taken for autoradiography and hematoxylin–eosin staining. Phosphor screens were exposed for ^{99m}Tc and ^{125}I, and images were processed. The MIBG image was subtracted from the methoxyisobutylisonitrile (MIBI) image and vice versa, and color tables were applied to the difference images and overlaid on the perfusion images. Quantitative analysis of the light image data was also performed. **Results:** Thirty-three sections from the last 3 experiments were analyzed. Acoustic damage from 30 laser channels was identified from the hematoxylin–eosin sections. Reduced MIBG relative to regional flow was seen in surrounding tissue corresponding to only 1 channel. There was no statistically significant difference in light units expressed as (MIBG − MIBI)/maximal MIBG value between laser channels and unmarked myocardial map regions. The regions identified from the color table on the map as low MIBG relative to MIBI were significantly lower than remaining laser channels and remaining myocardium. Mean light units for the regions with high MIBG relative to MIBI were significantly higher than the remaining laser channels and remaining myocardium. **Conclusion:** Using a high-resolution technique correlated with microscopic pathology in an animal model, there is negligible regional denervation 3 d after placement of endomyocardial laser channels.

Key Words: lasers; metaiodobenzylguanidine; mapping catheter; swine model

J Nucl Med 2002; 43:551–555

Received Aug. 1, 2001; revision accepted Dec. 12, 2001.

For correspondence or reprints contact: Lynne L. Johnson, MD, Rhode Island Hospital, Main Building, Room 208, 593 Eddy St., Providence, RI 02903.

E-mail: Lynne_Johnson@brown.edu

R wave voltage endomyocardial mapping with wall motion (NOGA, Biosense Webster; Cordis Corp., Johnson & Johnson, Miami, FL) is a new catheter-based imaging modality. The principle underlying the development of this technology is that the R wave amplitude correlates inversely with the percentage of transmural myocardial fibrosis (*1*). Several validation studies were performed using experimental animal models (*2–4*). The NOGA catheter mapping system can be used to guide endomyocardial laser therapy and direct gene delivery to the myocardium.

Increasing numbers of patients with end-stage ischemic heart disease are not candidates for revascularization because of previous surgery or poor vessels for grafting, angioplasty, or stenting. These patients who fail medical therapy are left with either disabling angina or ischemic heart failure (or both). Novel methods to revascularize the heart are under investigation. One method is placement of laser channels into the myocardium using either transmural or endocardial approaches. The concept that sinusoidal channels can connect cavitary blood with the myocardium to offer nutrient perfusion is an old one (*5*). The advent of laser technology presented a new approach to create myocardial channels. The CO_2 laser has been used to create transmural channels but cannot be catheter mounted. The holmium/yttrium-aluminum-garnet (Ho:YAG) laser has been adapted into a catheter-based system to deliver acoustic energy to the endocardium. More tissue damage occurs with the Ho:YAG laser compared with the CO_2 laser, and the proposed mechanism for revascularization using this approach is through angiogenesis stimulated by inflammatory cytokines released by local acoustic injury (*6,7*). Patients treated with either transmural or endocardial laser experienced relief of anginal symptoms within days of the procedures. It has been hypothesized that this early response may be attributed to denervation. It was the purpose of this experiment to investigate this hypothesis in a relevant animal model. Tissue assays for tyrosine hydroxylase are difficult to perform and subject to sampling error. Metaiodobenzylguanidine (MIBG) is an analog of the false trans-

mitter guanethedine (*8*), which is taken up by a type 1 mechanism in presynaptic vesicles similar to norepinephrine (*9,10*). Tagged with a radioiodine tag, it is used experimentally and clinically to image the sympathetic nervous system (*11,12*).

MATERIALS AND METHODS

Laser Therapy

For all experiments, conditioned castrated male juvenile swine weighing 20–30 kg were used. All experiments were performed within the guidelines of the National Institutes of Health for care and use of laboratory animals and with the approval of the Rhode Island Hospital Animal Care Committee. Animals were immobilized followed by induction using thiopental sodium (Pentothal; Abbott Laboratories, North Chicago, IL) in an ear vein for intravenous access and intubation. All surgical procedures were performed on completely anesthetized animals using inhalant anesthetics. Sterile procedures were followed on day 1. Cutdowns were performed on the left femoral artery that was used for pressure monitoring, blood gases, and NOGA mapping and laser. The baseline NOGA map and a 12-lead electrocardiogram were obtained. Direct myocardial laser therapy was performed placing 30 channels in the anterior wall (Fig. 1). The femoral sheath was removed to reestablish arterial circulation using vessel repair if necessary. After arterial bleeding stopped for at least 10 min, the incision was closed using Vicryl suture (Johnson & Johnson, Somerville, NJ) and surgical steel skin staples. The animal was allowed to awaken and returned to a recovery pen. Antibiotics and analgesics were given postoperatively.

After the animals had survived for 3 d they were sedated and injected with 37 MBq ^{125}I-MIBG followed 3 h later with a dose of 925–1,110 MBq ^{99m}Tc-sestamibi. The animals were killed 1 h later. The hearts were removed, perfusion fixed, and sliced into 1-cm slices. The slices best showing the laser holes were selected. These slices were frozen at −80°C. Three or four 30-μm-thick circumferential slices (divided into 4 sections: septal, anterior, lateral, inferoposterior) were taken using a microtome at −20°C and removed from the tissue block. Sections were mounted on slides and positioned on a phosphor screen (Cyclone; Packard Instruments, Meriden CT). Ten-micron serial sections were reserved for hematoxylin–eosin staining to identify the laser holes. The screen was exposed for 40 h for ^{99m}Tc. The plate was scanned and the image was captured. The plate was then stored for 3 d to allow all ^{99m}Tc to decay and was then developed for 10 d for the ^{125}I. The plate was rescanned and the second set of images was captured.

Data Analysis

The cross-sectional myocardial images were oriented the same way and displayed side by side to compare innervation (^{125}I-MIBG) and perfusion (^{99m}Tc-sestamibi). The digital images were processed using Image Pro 4.1 (Media Cybernetics, Silver Spring, MD). Background was subtracted from each image. Each image was then normalized to the hottest pixel. The MIBG image was subtracted from the methoxyisobutylisonitrile (MIBI) image and vice versa. Color tables were applied to the resulting images. The subtraction images were overlaid on the original images to create a map.

Corresponding sections stained with hematoxylin–eosin were examined under the microscope. The locations of laser damage to the endocardium were easily identified on the sections, and circles denoting their locations were transcribed to the corresponding slide image on the map.

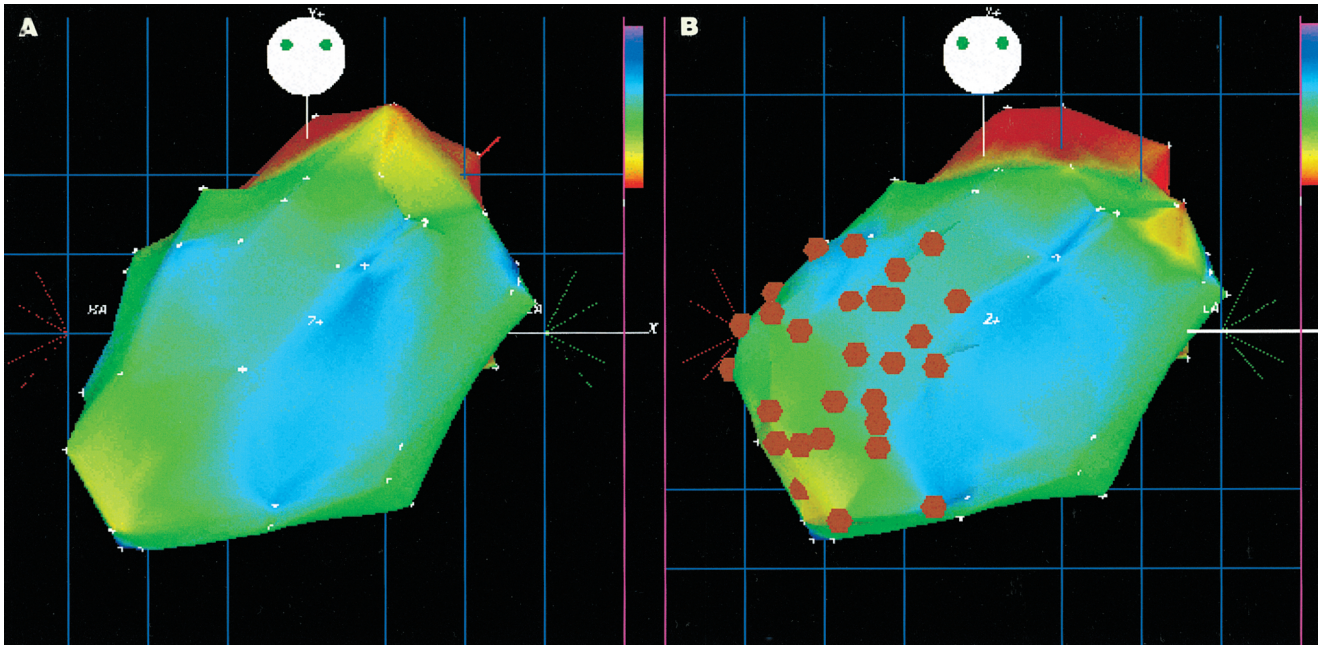

FIGURE 1. Display of 3-dimensional unipolar voltage maps in shallow left anterior oblique projection acquired using NOGA catheter mapping system. (A) Map was done at baseline before laser therapy and shows normal unipolar voltage. (B) Map was done during laser therapy. White points on left ventricular map represent mapping points, and orange dots represent sites of laser administration to endocardial surface of anteroapical wall. Color bars represent 5 (orange) to 15 (blue/purple) mV. White disk represents animal's head and is placed for orientation.

Quantitative analysis of the light image data were also performed. In addition to regions of interest (ROIs) corresponding to the laser channels, ROIs were drawn around areas on the computer-generated subtraction/overlay map identified as low MIBG to MIBI counts, high MIBG to MIBI counts, and other representative regions were selected from the remaining myocardium. Light units for ROIs were expressed as (MIBG − MIBI)/maximal MIBG value (difference/maximal) and compared using a 2-tailed unpaired *t* test.

RESULTS

Maps and Laser Therapy

Four experiments were performed. A minimum of 60 mapping points was acquired per animal. The unipolar maps and the regional contraction maps were within normal limits established in our laboratory for swine. Between 20 and 30 laser channels were placed per animal (Fig. 1). The acoustic damage sites corresponding to the laser sites on the map were identified in the endocardium of the hearts removed after at killing the animals.

Autoradiography

Data from the first experiment could not be used because of low counts or poor exposure on the MIBI screens. For the last 3 experiments, corresponding left ventricular segment slices developed for ^{125}I-MIBG, ^{99m}Tc-sestamibi, and hematoxylin–eosin staining were compared. Thirty-three sections were analyzed. Thirty laser holes were identified on the hematoxylin–eosin sections and located on the MIBG/MIBI maps. Nine sections had no laser holes. Of the 30 laser holes identified, only 1 was associated with reduced MIBG uptake compared with MIBI uptake defined as a confluent area of adjacent pixels (Fig. 2).

Mean light units for ROIs expressed as difference/maximal for the 4 regions identified as low MIBG (only 1 laser channel) was 0.19 ± 0.15 and for the 10 regions with high

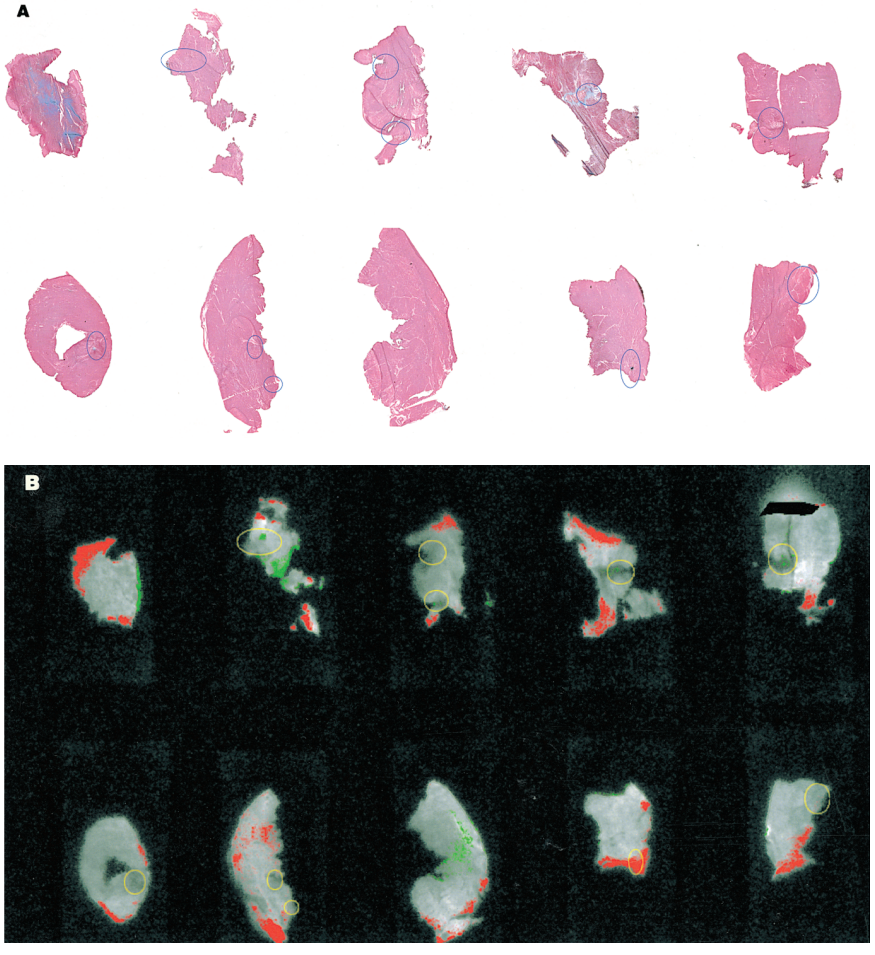

FIGURE 2. Hematoxylin–eosin staining (A) and autoradiograms (B) from 1 experiment. Each tissue section was mounted on a slide. Sections were selected to include sites of laser treatment. (A and B) Ten sections displayed in 2 rows. (A) Regions of laser channels are marked by blue circles. (B) Phosphor screen captured image of perfusion tracer (^{99m}Tc-sestamibi) is displayed in gray scale and superimposed are results of 2 subtraction processes. Red pixels represent relatively higher MIBG than MIBI and green pixels represent relatively lower MIBG than MIBI when compared with remaining myocardium (gray). Yellow circles correspond to locations of laser holes identified from hematoxylin–eosin sections. Only 1 laser site with confluent green pixels showed reduced MIBG (second section from right in second row).

MIBG relative to MIBI was 0.53 ± 0.07. Both were significantly different ($P < 0.001$ and $P = 0.02$, respectively) from the mean light unit values for the laser channels (0.48 ± 0.06) and remaining myocardium (0.45 ± 0.05). The latter 2 values were not significant ($P = 0.96$).

DISCUSSION

In the 1930s, Wearn et al. (*5*) described naturally occurring arteriosinusoidal vessels connecting coronary arteries with the left ventricular chamber in human cadaveric hearts. These observations led to the concept that myocardial perfusion could be improved by mechanically creating new sinusoidal channels in the myocardium. In 1965, Sen et al. (*13*), using a canine infarct model, created transmural myocardial channels using a blunt instrument and found reduction in infarct size compared with controls. The development of laser technology presented the opportunity to make transmyocardial channels using photothermal ablation. Several surgical groups have performed thoracotomies and used transmyocardial revascularization with CO_2 lasers applied from the epicardium in patients with nonrevascularizable vessels and reported improvement in symptoms and evidence for enhanced myocardial perfusion by SPECT (*14,15*). A randomized trial of CO_2 laser revascularization versus optimal medical therapy was performed, and preliminary analyses support these observations (*15*). Results also show that the beneficial effect persists for at least 2 y after the procedure.

Kwong et al. (*16*) showed in a canine model that creation of transmural laser channels results in denervation of the treated myocardium. These experiments indicated the elimination of visceral afferent nerve function as assessed by epicardial bradykinin, a potent algesic agent that stimulates cardiac afferent pain fibers, and the disappearance of the neural-specific enzyme tyrosine hydroxylase in the laser-treated regions of the heart. Al-Sheikh et al. (*17*) used PET imaging with ^{13}N-ammonia for perfusion and ^{11}C-hydroxyephedrine for sympathetic innervation. He showed in 8 patients that the improvement in angina class between baseline and follow-up posttransmural laser channels was associated with an increase in sympathetic defects but not rest or stress perfusion defects. Hughes et al. (*18*) recently showed in a hibernating swine model that at 6 mo lased segments were reinnervated. Immunohistochemistry was positive for tyrosine hydroxylase in the lased segments, hibernating nonlased segments, and normal segments. Western blot analysis indicated no difference in the tyrosine hydroxylase protein concentration between any of the groups. These studies suggest that the early denervation seen with transmural laser channels may not be sustained at 6 mo.

The CO_2 laser, which is a continuous wave laser, produces a photothermal ablative effect that is confined to a thin zone and clean channel borders. This laser cannot be transmitted by fiber optics and cannot be used for catheter-based applications. However, the Ho:YAG laser was adapted for use in the catheter-based direct myocardial revascularization technique to create endomyocardial channels using the electromechanical endocardial mapping system (NOGA, Biosense Webster) (*19,20*). These lasers use short laser pulses that produce photothermal and photoacoustic (shock-wave) tissue effects in contrast to the cleaner and straighter channel borders produced by the CO_2 laser; the Ho:YAG laser produces large zones of collateral tissue injury and irregular channel borders. The NOGA system consists of several components: a triangular location pad with 3 coils generating an ultra-low magnetic field, a stationary reference catheter with magnetic field sensor, and a processing unit. The mapping catheter has an endocardial electrode (records unipolar or bipolar signal) and a magnetic field (location) sensor. The navigation mapping catheter sensor determines its precise location through triangulation off of the 3 coils in a manner similar to the Global Positioning System used by mariners and in general and commercial aviation. A computer workstation processes information recorded from the navigation mapping catheter and constructs a 3-dimensional left ventricular image. The left ventricular endocardial surface geometry can be displayed in color-coded maps according to R wave voltage or mechanical function (local shortening recorded by change in the tip position from diastole to systole). R wave amplitude is reduced by scar and ischemia.

Cardiac visceral afferent nerve fibers thought to convey the pain of angina pectoris and the sympathetic efferent fibers travel in a subepicardial location adjacent to the coronary vasculature (*21*). It is possible there is less cardiac denervation with a catheter-based endocardial approach. One experimental study showed reduced afferent nerve function and reduced tissue tyrosine hydroxylase 2 wk after nontransmural laser treatment in a canine model (*16*). Another group of investigators did not find any reduction in tissue growth factor peptide nerve growth factor at 5 wk in a porcine model (*7*). The development of phosphor screen technology has improved the spatial resolution for uptake and distribution of this tracer in whole-heart slices. Dae et al. (*12*) have shown in a canine model that MIBG/perfusion functional maps accurately displayed regional distribution of sympathetic innervation. MIBG autoradiography using phosphor screens offered the opportunity to evaluate regional innervation over entire rings of myocardium and overcome sampling errors from tissue assays.

CONCLUSION

This study further developed the methodology of high-resolution autoradiography to map regional innervation in large animals and showed the absence of early myocardial denervation soon after endomyocardial laser treatment. The results of this study are consistent with the known anatomic routes of afferent nerve fibers and are also consistent with the outcome of the multicenter double-blind placebo-con-

trolled trial of endomyocardial laser treatment that showed a very strong placebo effect (*22*).

REFERENCES

1. Ben-Haim SA, Osadchy D, Schuster I, Gepstein L, Hayam G, Josephson ME. Nonfluoroscopic, in vivo navigation and mapping technology. *Nature Med*. 1996;2:1393–1395.
2. Gepstein L, Hayam G, Ben-Haim SA. A novel method for non-fluoroscopic catheter-based electroanatomical mapping of the heart: in vitro and in vivo accuracy results. *Circulation*. 1998;95:1611–1622.
3. Kornowski R, Hong MK, Leon MB. Comparison between left ventricular electromechanical mapping and radionuclide perfusion imaging for detection of myocardial viability. *Circulation*. 1998;98:1837–1841.
4. Kornowski R, Hong MK, Gepstein L, et al. Preliminary animal and clinical experiences using an electromechanical endocardial mapping procedure to distinguish infarcted from healthy myocardium. *Circulation*. 1998;98:1116–1124.
5. Wearn J, Mettier S, Klumpp T, Zschiesche L. The nature of the vascular communications between the coronary arteries and the chambers of the heart. *Am Heart J*. 1933;9:143–164.
6. Schaper W, Ito WD. Molecular mechanisms of coronary collateral vessel growth. *Circ Res.* 1996;79:911–919.
7. Fuchs S, Vodovotz Y, Leon MB, Kornowski R. Laser myocardial revascularization enhances expression of angiogenic cytokines in a porcine model of chronic myocardial ischemia [abstract]. *J Am Coll Cardiol.* 1999;33:342A.
8. Short JH, Darby TD. Sympathetic nervous system blocking agents. III. Derivatives of benzylguanidine. *J Med Chem.* 1967;10:833–840.
9. Wieland DM, Wu JL, Brown LE, Mangner TJ, Swanson DP, Bierwalthers WH. Radiolabeled adrenergic neuron-blocking agents: adrenomedullary imaging with (131-I) iodobenzylguanidine. *J Nucl Med.* 1980;21:349–353.
10. Nakajo M, Shimabukuro K, Miyji N, et al. Iodine-131 metaiodobenzylguanidine intra- and extra-vesicular accumulation in the rat heart. *J Nucl Med.* 1986;27: 84–89.
11. Kline RC, Swanson DP, Wieland DM, et al. Myocardial imaging in man with I-123 metaiodobenzylguanidine. *J Nucl Med.* 1981;21:129–132.
12. Dae MW, O'Connell JW, Botvinick EH, et al. Scintigraphic assessment of regional cardiac adrenergic innervation. *Circulation.* 1989;79:634–644.
13. Sen P, Udwadia T, Kinare S, Parulkar G. Transmyocardial acupuncture: a new approach to myocardial revascularization. *J Thorac Cardiovasc Surg*. 1965;50: 181–189.
14. Frazier OH, March RJ, Horvath KA. Transmyocardial revascularization with a carbon dioxide laser in patients with end-stage coronary artery disease. *N Engl J Med*. 1999;341:1021–1028.
15. Allen KB, Dowling RD, Fudge TL, et al. Comparison of transmyocardial revascularization with medial therapy in patients with refractory angina. *N Engl J Med*. 1999;341:1029–1036.
16. Kwong KF, Schuessler RB, Kanellopoulus GK, Saffitz JE, Sundt TM. Nontransmural laser treatment incompletely denervates canine myocardium. *Circulation*. 1998;98(suppl):II-67–II-72.
17. Al-Sheikh T, Allen KB, Straka SP, et al. Cardiac sympathetic denervation after transmyocardial laser revascularization. *Circulation*. 1999;100:135–140.
18. Hughes CG, Baklanov DV, Annex BH, et al. Denervation is not the long-term mechanism of action of transmyocardial laser revascularization [abstract]. *Circulation*. 1999;100:I-249.
19. Kornowski R, Hong MK, Leon MB. Current perspectives on direct myocardial revascularization. *Am J Cardiol*. 1998;81:E44–E48.
20. Kornowski R, Hong MK, Leon MB. Direct myocardial revascularization in ischemic heart disease. *Int J Cardiovasc Interven*. 1998;1:3–9.
21. White JC. Cardiac pain: anatomic pathways and physiologic mechanisms. C*irculation*. 1957;16:644–655.
22. Leon MB, Baim DS, Moses JW, et al. A randomized blinded trial comparing percutaneous laser myocardial revascularization (using Biosense LV mapping) vs placebo in patients with refractory coronary ischemia [abstract]. *Circulation*. 2000;102:II-565.

SOCIETY OF NUCLEAR MEDICINE